Phylogenetic and pathogenic characterization of Mauginiella scaettae as the causal agent of date palm (Phoenix dactylifera L.) inflorescence rot in southeast of Algeria

Bensaci, Messaoud B.; Toumatia, Omrane; Bouras, Noureddine; Rahmania, Fatma; Douglas, Brian; Wade, Stephen; Griffith, Gareth W.; Mur, Luis A.J.

Published in:
Physiological and Molecular Plant Pathology

DOI:
10.1016/j.pmpp.2023.102062

Publication date:
2023

Citation for published version (APA):
Bensaci, M. B., Toumatia, O., Bouras, N., Rahmania, F., Douglas, B., Wade, S., Griffith, G. W., & Mur, L. A. J. (2023). Phylogenetic and pathogenic characterization of Mauginiella scaettae as the causal agent of date palm (Phoenix dactylifera L.) inflorescence rot in southeast of Algeria. *Physiological and Molecular Plant Pathology*, *127*, Article 102062. https://doi.org/10.1016/j.pmpp.2023.102062

Physiological and Molecular Plant Pathology 127 (2023) 102062

Contents lists available at ScienceDirect

Physiological and Molecular Plant Pathology

journal homepage: www.elsevier.com/locate/pmpp

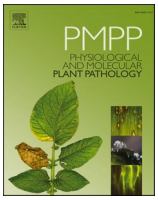

Phylogenetic and pathogenic characterization of *Mauginiella scaettae* as the causal agent of date palm (*Phoenix dactylifera* L.) inflorescence rot in southeast of Algeria

Messaoud B. Bensaci [a,b,c,**], Omrane Toumatia [d], Noureddine Bouras [d,e], Fatma Rahmania [c], Brian Douglas [f,1], Stephen Wade [f], Gareth W. Griffith [f], Luis A.J. Mur [f,*]

[a] Faculté des Sciences Biologiques, Laboratoire de Recherche sur les Zones Arides, Université des Sciences et de la Technologie Houari Boumediene, B.P.32. El - Alia, Bab-Ezzouar, Alger, Algeria
[b] Ecole Normale supérieure de Ouargla, Département des Sciences naturelles, Ouargla, 30000, Algeria
[c] Laboratoire de Protection des écosystèmes en Zones Arides et Semi Arides, Université Kasdi Merbah-Ouargla, 30000, Ouargla, Algeria
[d] Laboratoire de Biologie des Systèmes Microbiens (LBSM), Ecole Normale Supérieure de Kouba, Alger, Algeria
[e] Département de Biologie, Faculté des Sciences de la Nature et de la Vie et Sciences de la Terre, Université de Ghardaia, Ghardaïa, Algeria
[f] Department of Life Sciences (DLS), Edward Llwyd Building, Aberystwyth University, Penglais, Aberystwyth, Ceredigion, SY23 3DA, Wales, UK

ARTICLE INFO

Keywords:
Date palm
Inflorescence rot
Mauginiella scaettae
ITS region
FTIR

ABSTRACT

Inflorescence rot is a devastating disease of date palm (*Phoenix dactylifera* L.) but has not been extensively characterised. *Mauginiella scaettae* Cav. 1925 (Pleosporales; Ascomycota), causal agent of this disease, was isolated from infected male and female inflorescences of date palm from different oases in the southeast of Algeria: Ouargla (strains OU1, OU2, OU3), Tougourt (strains TO1, TO2), Hadjira (strain HA), Oued (strains OE1, OE2), Ghardaia (strain GA) and Biskra (strain BI). Each strain of *M. scaettae* was used to infect healthy male inflorescence of date palms to satisfy Koch's postulates but follow on assessments were based on GA. Phylogenetic reconstruction using the rRNA sequence data (ITS and LSU regions) found no intraspecific differentiation of strains and confirmed the placement of *M. scaettae* within the family Phaeosphaeriaceae. Fourier Transform Infrared spectroscopy (FTIR) metabolite fingerprinting discriminated between fungal strains originating from male and female inflorescences. Scanning electron microscopy (SEM) characterisation of the infection processes for *M. scaettae* in both male and female inflorescences suggested a preference for stomatal entry. Our characterisation provides new insights into this inflorescence rot to allow better detection and management of the disease.

1. Introduction

Date palm (*Phoenix dactylifera* L.) is a dioecious tree species which is one of the most important crops in North Africa. For example, date production in Algeria surged from 206 MT in 1990 to 1152 MT tonnes in 2020 [1]. Quantitatively Algeria provides 12.2% of world production [1], it is the first producer of the Deglet-Nour variety which is among the most popular varieties in the world. However, the date palm sector has been compromised by loss of palm groves by severe drought or being buried under sand dunes (Bouguedoura et al., 2015). Losses due to pests and pathogens are also significant (Carpenter, & Elmer, 1978; [2,3]; Abdullah et al., 2005) with serious damage linked to Bayoud disease which infects palm fronds and is caused by *Fusarium oxysporum* f. sp. *albedinis* (Bouguedoura et al., 2015)

One of the major diseases of date palm is inflorescence rot (known as Khamedj disease in North Africa). Inflorescence rot is a major factor that limits yield, which in severe cases can destroy around 50–80% of the date palm inflorescences. The disease is most devastating during

* Corresponding author. Department of Life Sciences (DLS), Edward Llwyd Building, Aberystwyth University, Penglais, Aberystwyth, Ceredigion, SY23 3DA, Wales, UK.
** Corresponding author. Faculté des Sciences Biologiques, Laboratoire de Recherche sur les Zones Arides, Université des Sciences et de la Technologie Houari Boumediene, B.P.32. El - Alia, Bab-Ezzouar, Alger, Algeria.
E-mail addresses: bensacimessaoudbachagha@gmail.com (M.B. Bensaci), lum@aber.ac.uk (L.A.J. Mur).
[1] Current address: Bento Bioworks Ltd., 5 Hancock Road, London E3 3DA.

https://doi.org/10.1016/j.pmpp.2023.102062
Received 3 March 2023; Received in revised form 30 May 2023; Accepted 31 May 2023
Available online 6 June 2023

extended periods of heavy rain (up to two months) before the emergence of the spathes which are bracts covering the developing flowers. The symptoms are more apparent on the internal face of the spathes and infections occur early in the young inflorescence when the spathe is still hidden in the leaf bases (Carpenter & Elmer, 1978). Disease transmission occurs through the contamination of male inflorescences during the pollination period (Al-Ani, El-Behadili, Majeed, & Majeed, 1971). Disease can persist on the trees and cause rotted inflorescences for several years.

Mauginiella scaettae is frequently isolated infected inflorescences of date palm and, as such, is thought to be the causal agent. Date palm is inflorescence rot was first reported by Refs. [4,5] in Cyrenaica, Libya and throughout the region (Chabrolin, 1928; [6–8]; Calcat, 1959; [9] including Egypt [10], the Arabian Peninsula (Abu Yaman & Abu Blam, 1971; [2]), Iraq [11]; Al-Ani, El-Behadili, Majeed, & Majeed, 1971) and Southern Spain (Abdullah et al., 2005). However, other fungi such as Fusarium *oxysporum* Schldl. emend. Snyder and Hansen, Fusarium *moniliforme* Sheld. Aggregate, Fusarium *solani* (Mart.) Appel and Wollenw. aggregate Snyder and Hansen, *Thielaviopsis paradoxa* (Dade) C. Moreau. and *Trichothecium roseum* (Pers.) Link, have also been commonly found associated with rotten date palm inflorescences (Brown & Butler, 1938; El-Behadili, Mawlood, & Diwan,1977; [9].

This study aimed to identify the fungi that are associated with date palm inflorescence rot in Algeria and to confirm that *M. scaettae* is the causal agent. Additionally, electron microscopy was used to determine how the fungus colonises host tissues.

2. Materials and methods

2.1. Purification of fungal strains from diseased date palm inflorescences

Sampling of diseased male and female date palm inflorescences was undertaken in March–May 2012 in southeast of Algerian oasis, Ouargla, Touggourt, Hadjira, Oued, Biskra, Ghardia (Supplementary Fig. 1). These areas were identified following previous reports of inflorescence rot.

Fungal strains were isolated from ~1 cm^2 tissue samples from infected inflorescences following surface-sterilization with 90% ethanol or 10% sodium hypochlorite. Sterily dissected parts were placed in Petri dishes containing 10% sodium hypochlorite solution for 10 min, and then washed repeatedly in sterilized water before drying between sheets of sterile blotting paper. Samples were transferred to Petri dishes with Potato Dextrose Agar (PDA, Oxoid, UK) and incubated at 22 °C in the dark. No investigation of how incubation temperature could impact on the strains that would be isolated from the infected samples was carried out. Pure cultures were obtained by repeated isolation of each emergent fungal mycelium.

For micro-morphological observations, mycelial samples were obtained from cultures grown on PDA and imaged using a Nikon Coolpix digital camera installed on an Olympus BX50 light microscope. The description of the mycelium and arthroconidia follows established terminologies (Chabrolin, 1930; Abdullah et al., 2005).

2.2. Pathogenicity test

Arthroconidia from each strain (Table 1) were grown on PDA were used for pathogenicity assays, and with a suspension of arthroconidia (10^5 spores.ml-1) prepared in sterile water. Healthy (male) spathes were surface-sterilized with 95% ethanol, and the upper external surface of the spathe was removed so that the flowers and strands were exposed. These were inoculated by spraying with 20 mL of the arthroconidia suspension per inflorescence, placed in commercially obtained sterile plastic bags (Fisher Scientific, UK) and incubated at 22 °C in the dark. Spathes were examined for symptoms after 1 week.

Table 1
Ten sites in South-East of Algeria origin of the inflorescence rot in date palm.

Sample origin	Grid reference	Isolate code	Date palm Varity	sex	Tree age (Years)	Accession number
Biskra	N34.84, E5.72	BI	Dokar	Male	52	KT587190
ElHadjira	N32.62, E5.51	HA	Dokar	Male	30	KT587192
ElOued	N33.37, E6.84	EO1	Ghars	Female	60	KT587191
ElOued	N33.37, E6.84	OE2	Ghars	Female	65	KT587187
Ghardaïa	N32.51, E3.63	GA	Ghars	Female	35	KT587194
Ouargla	N31.96, E5.31	OU1	Dokar	Male	50	KT587185
Ouargla	N31.96, E5.31	OU2	Dokar	Male	36	KT587186
Ouargla	N31.96, E5.31	OU3	Dokar	Male	45	KT587193
Tougourt	N33.10, E6.00	TO1	Dokar	Male	40	KT587188
Tougourt	N33.10, E6.00	TO1	Dokar	Male	47	KT587189

2.3. Re-isolation of the pathogen

To satisfy Koch's Postulates, parts from inoculated inflorescences (spathe, flowers and stands) exhibiting disease symptoms were surface-sterilized (5 min) with 5% sodium hypochlorite, washed three times with sterile distilled water and plated on PDA. Plates were incubated at 22 °C and the subsequent growth of the pathogen was recorded.

2.4. Genomic DNA extraction and PCR amplification and DNA sequencing

Genomic DNA was extracted from fungal mycelia using a QIAGEN DNeasy Plant mini kit (Qiagen, Manchester, UK) following the manufacturer's protocol. The universal primers ITS1F (CTTGGTCATTTAGAGGAAGTAA) and ITS4 (TCCTCCGCTTATTGATATGC) primers were used to amplify the ITS region and the primers LR0R (ACCCGCTGAACTTAAGC) and LR6 (CGCCAGTTCTGCTTACC) for the LSU region [12] For both amplicons the amplification was conducted as follows: 4 μL of 10X Thermo buffer, 4 μL dNTP (0.2 mM final concentration), 3.2 μL $MgCl_2$ (2 mM), 0.1 μL (0.5U) *Taq* DNA polymerase, 2 μL of each primer (0.5 μM), 20 μL dH_2O, and 20 μL DNA template in a total volume of 40 μL. The polymerase chain reaction (PCR) was performed in a GenAmp 9700 thermal cycler (Mycycler, Bio-Rad, UK) using the following conditions: 4 min at 94 °C, 35 cycles of 50 s at 94 °C, 60 s of annealing at 56 °C and 50 s of extension at 72 °C; followed by final extension for 5 min at 72 °C. The PCR products were separated on a 1.2% agarose gel and purified using QIAquick PCR columns (Qiagen, Manchester, UK). Samples were sequenced in a 377 Agilent sequencer (Fisher Scientific, UK) and the sequences were submitted to the NCBI GenBank database (Table 1).

2.5. Phylogenetic analyses

Sequence management was conducted within the Geneious Prime bioinformatics package [13]. Sequences were aligned using MAFFT [14] using default setting and trimmed to remove flanking 18S/28S sequences. Phylogenetic reconstruction was conducted using PhyML (Maximum Likelihood) and the GTR (Generalised time reversible) substitution model with 1000 bootstrap replications [15].

2.6. Fourier transform-infrared (FTIR) spectroscopy

Strain differences were examined using FTIR metabolite fingerprinting. Fungal mycelium was cultured in Potato Dextrose Broth (Oxoid, UK), centrifuged and spotted on to a silica plates for assessment using FTIR reflectance spectroscopy.

The FTIR reflectance spectra were obtained using a Bruker Vertex 70 (Bruker Optics; http://www.brukeroptics.com/) as described in Ref. [16]; but using a mercury–cadmium telluride (MCT) detector to measure sample reflectance. Data were analysed using MATLAB version 6.5 (MathWorks; http://www.mathworks.co.uk/). In-house algorithms were used to convert the resultant spectra into absorbance readings. The CO_2 peaks were replaced with a smooth trend using an in-house code, and the spectra were normalised to total absorbance [17].

Principal Component Analysis (PCA) and Principal Component – Discriminant Function Analyses (DFA) were used as described in Allwood et al. (2006) and followed accepted Metabolomics Standards Initiative (MSI) standards [18]. PCA reduces the dimensionality of multivariate data whilst preserving most of the variance following which DFA is used to discriminate between groups on the basis of the retained PCs and the *a priori* knowledge of class structures within the datasets [19,20]. This process eliminates the analysis bias at all events.

2.7. Staining and microscopy

For scanning electron microscopy (SEM), freeze-substitution was carried out using a Leica EM AFS unit. Substitution fluids were pre-cooled to −80 °C before the frozen tissue was transferred into them for substitution. Transfer was performed using suitably pre-cooled and insulated tools. Critical point drying of freeze-substituted samples was performed from 100% acetone at 10 °C, in a Polaron E3000 unit, utilizing liquid carbon dioxide. Specimens were cooled to liquid nitrogen temperature and fractured, in the plane parallel or perpendicular to the tibial plateau, under vacuum using the steel blade in a modified Polaron freeze fracture unit. The specimens were then brought back to room temperature whilst being kept under vacuum to prevent artefacts forming due to water condensing on the cold specimens, and they mounted on specimen stubs. Specimen coating, in all cases, was carried out in a Polaron E5000 sputter coating unit with a cooled specimen holder, utilizing a platinum target and argon gas to provide approximately 10 nm coating. High resolution images were also obtained on a Hitachi 4700 Scanning Electron Microscope.

3. Results

3.1. Date palm inflorescence rot symptom on its natural host

The disease is generally first observed in late winter or early spring as the spathes begin to emerge. Infected spathes of male date palm (Fig. 1 A, B) first exhibit rot symptoms when they begin to emerge in early spring. Typically, these are seen as necrotic spots and patches on the spathe (Fig. 1C). As the spathe matures and splits open, white mycelia is seen covering the flowers, especially at the top of the spathe (Fig. 1D). Tissue necrosis is progressively observed inside the spathe, while hyphae are visible on the outside of the spathe (Fig. 1E). In female inflorescences, the flowers erupt rapidly from the spathe (Fig. 1F). Necrotic (rot) symptoms are observed from flower emergence in late spring onwards, as pollination is in progress. Generally, symptoms begin as a white mycelial mass attacking the flowers (Fig. 1G). The spathes split to reveal partial to near complete coverage of the flowers with white mycelium. As the infected flowers emerge, the areas previously covered with white mycelium become necrotic (Fig. 1H), killing the mature flowers (Fig. 1I).

3.2. Culturing of fungi from inflorescence rot disease date palm

Explants from date palm inflorescences were obtained from trees exhibiting inflorescence rot, including trees of both sexes, ranging in age from 35 to 60 years (Table 1). Fungal colonies emerging from surface-sterilized tissue explants (infected and symptomatic) were white (Fig. 2A) and similar to the growth seen on infected spathes (Fig. 1). Repeated subculture led to the isolation of a series of strains from each spathe, all of which appeared to have an identical white appearance. Isolates formed colonies up to 5 cm diameter after 10 days of growth at 22 °C on PDA (Fig. 2B). The underside of these colonies became light olive green with darker edges after prolonged culture. The selected representative strains for each spathe were designated according to their origins (Table 1).

Each strain was examined under the microscope light to reveal identical hyphal and arthroconidial morphologies (Fig. 2C). The mycelium was hyaline that was branched septate and produced 1- or 2-celled hyaline conidia, as long chains. Arthroconidial dimensions were 12-60 x 8–12 μm. Immersed hyphae were 1.5–2.5 μm and aerial 3–4 μm wide. Arthroconidia were produced by segmentation of aerial hyphae (Fig. 2C: h). This led to the production of unicellular non-septate conidia (Fig. 2C a1) or multicellular septate arthroconidia (Fig. 2C: a2, a3 and a4).

3.3. Pathogenicity test

Parts of the detached inflorescence (flowers, stands and spathes) were inoculated with spore suspensions of each *M. scaettae* strains Data are provided for strain GA as this provided typical responses. Clear inflorescent rot symptoms (Fig. 3A) were visible on all of these after incubation for 7 days. Arthroconidia from artificially inoculated inflorescence were plated out on PDA and grew into colonies identical to those isolated from naturally infected tissues (Fig. 3B).

3.4. Phylogenetic analyses

Confirmation of the identity of the isolated fungal strains was obtained sequencing of the ITS and partial LSU region of the rRNA operon. The finalised sequences are deposited in GenBank (KT587185-KT587194; Table 1). Each ITS sequence was identical and also the same as *M. scaettae* strains from Spain (AY965895) and Iraq (MH857770), thereby confirming the identity of these isolates and the absence of any intraspecific polymorphism within the hitherto analysed *M. scaettae* populations. Apart from other *M. scaettae* ITS sequences, the nearest BLAST search results were very distant (<92% sequence identity), with these hits all to various genera within Phaeosphaeriaceae.

A more detailed phylogenetic reconstruction using a combined ITS-LSU alignment found strong support for placement of *Mauginiella* within Phaeosphaeriaceae (Fig. 4). *Mauginiella* was placed close to the genera *Populocrescentia* and *Leptospora* and *Phaeosphaeriopsis*, consistent with the findings of Li et al. (2016) and [21]. However, bootstrap support for this placement was not high and phylogenetic reconstruction using additional loci would be needed for more accurate placement.

3.5. Fourier transform infrared spectroscopy (FTIR) analyses

Fungal samples were assessed using FTIR and the derived spectra showed variation between samples (Fig. 5A), which was analysed using chemometric methods. PCA of normalised absorbance data failed to identify any clear inter-strain differences but a supervised approach, Discriminant Function Analysis (DFA), where the algorithm was given *a priori* information of the classes of data was more informative. DFA based on 4 principal components (PC) explaining 96.5% of the total variation now were able to suggest some differences between the strains (Fig. 5B). Across DF2, two clusters of strains could be observed, and these corresponded to strains originated from either male or female inflorescences (Fig. 5B).

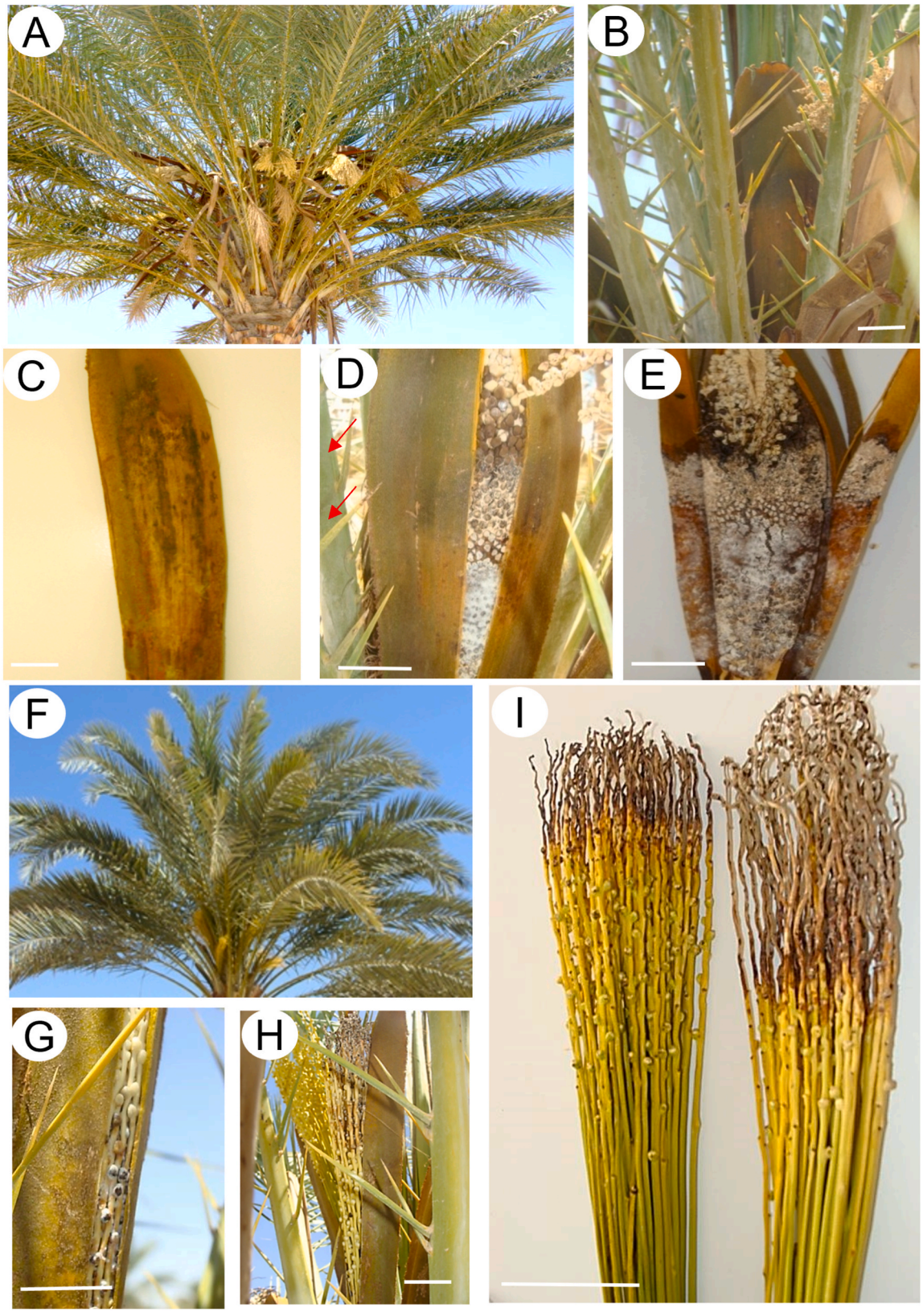

Fig. 1. Symptoms of date palm inflorescence rot caused by *Mauginiella scaettae*. (A) Male date palm with (B) male inflorescences with the spathe cover (bar = 10 cm). (C) Necrotic symptoms symptomatic of inflorescence rot (arrowed), as seen on the outside of the male spathe (bar = 5 cm) with (D) white mycelial development within the male spathe (bar = 2 cm). (E) white mycelial development and necrosis is eventually observed both within and outside the infected male spathe (bar = 5 cm). (F) healthy female date palm exhibiting the emergence of female flowers. (G) white mycelial development within inflorescence rot exhibiting female spathe (bar = 2 cm) which (H) is associated with necrotic symptoms as the flowers emerge (bar = 10 cm) and (I) kills the flowers at the tips (bar = 5 cm).

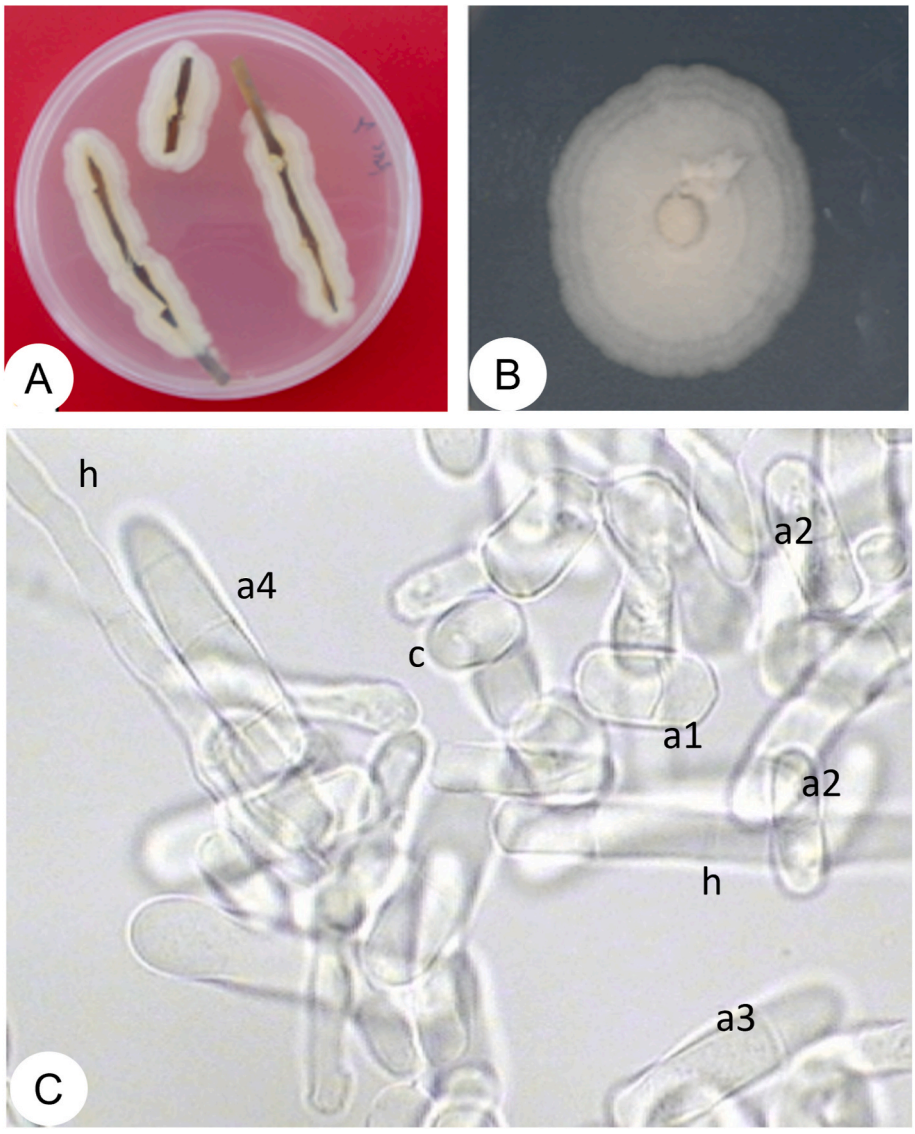

Fig. 2. Culture and light microscopic analysis of fungal strains isolated from diseases male and female date palm spathe. (A) The emergence of white fungal mycelia from explants of inflorescence rot exhibiting spathe. (B) After many rounds of sub-culture, single strains of white fungal colonies were isolated. (C) light microscopic analysis of fungal strain morphologies showing hyphae (h), and one (a1), two (a2), three (a3) and four-celled (a4) arthroconidia. Magnification 300x

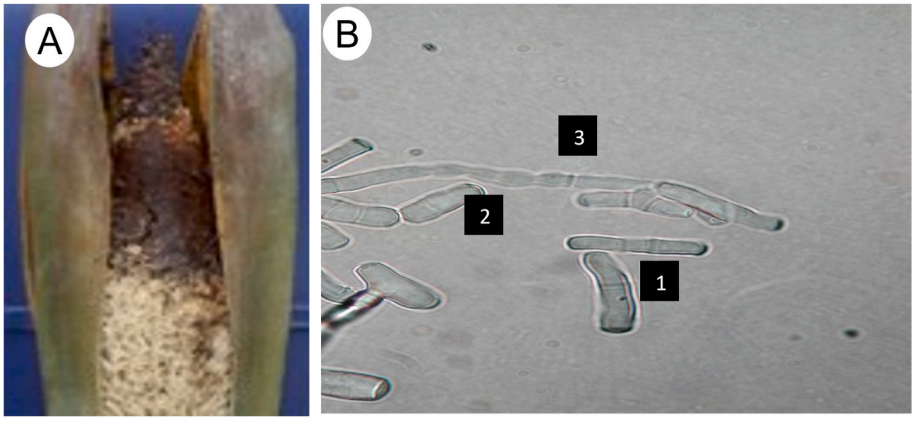

Fig. 3. Date palm spathe 1 weeks after artificial inoculation with *Mauginiella scaettae* (strain GA). (A) Opened spathe showing symptoms at the top. (B) Pure culture *Mauginiella scaettae* was re-isolated from all artificially inoculated parts: 1- from stand, 2-from flower, 3- from spathe. (C) Light microscopic analysis of GA strain morphologies showing hyphae and black boxed 1, a single celled arthroconidium; black boxed 2 – two celled arthroconidia tow cells, black boxed 3- three celled arthroconidia three cells. Magnification 100x.

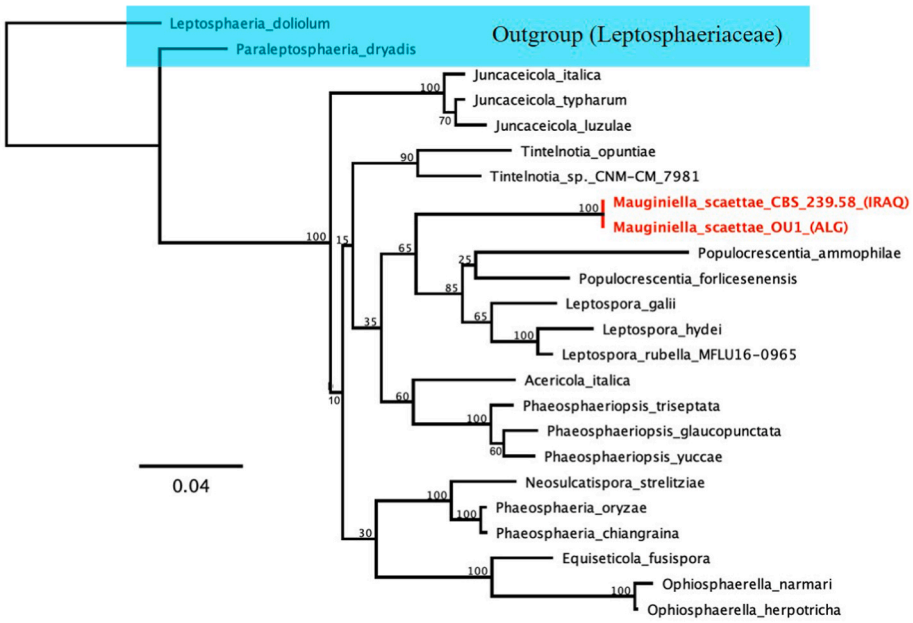

Fig. 4. Maximum likelihood tree based on concatenated ITS and LSU sequences (1387 bp alignment) for *Mauginiella* and other members of the family Phaeosphaeriaceae using *Leptosphaeria and Paraleptosphaeria* (Leptosphaeriaceae) as outgroup taxa. The backbone of the tree and clade assignation are based on the data of [21]. Values at nodes indicate bootstrap percentages (1000 replicates). Scale bar indicate numbers of substitutions per site.

3.6. Characterisation of the infection strategy of Mauginiella scaettae

In order to determine the infection strategy employed by *M. scaettae* disease, inflorescences were examined using SEM. The diseased spathes were covered with arthroconidia, identical to those formed in pure cultures of *M. scaettae* (Fig. 6A). Where arthroconidia were observed to have germinated, the resulting infection hyphae were observed on several occasions to penetrate the host via stomata (Fig. 6B). Other routes of entry into host tissues were not observed.

4. Discussion

Inflorescence rot is one of the most devastating diseases of date palm and as *M. scaettae* had been isolated from the infected both spathes of male and female date palm, it was suggested to be the causal agent. Such attributions were made before the advent of modern molecular approaches to fungal identification. However, in our investigations *M. scaettae* was the only fungus isolated from both male and female date palm inflorescences.

Symptoms of the disease were seen on all parts of the inflorescences, which includes brownish or rusty areas visible on the non-opened spathe after the pathogen has already invaded the floral tissues and in agreement with previous reports [4,5]. These tissues were used to isolate associated fungal strains. After 10 days of growth on PDA at 22 °C only white fungal colonies were observed, composed of branched hyaline septate hyphae. This is consistent with published descriptions of *M. scaettae*, whose mycelia and arthroconidia suggested it to be an anamorph of an unknown ascomycete [22].

The mechanism by which *M. scaettae* infects the host, is consistent with a hemibiotrophic strategy. Our observations suggest that *M. scaettae* targets stomata to penetrate its host. Such a strategy is also a feature of biotrophic pathogens such as rusts, where after spores land on the leaf surfaces, a germ tube forms which grows towards the stomata. This then forms an appressorium over the stomatal guard cells to penetrate the stomata and forms a microscopically visible haustorium in the substomatal cavity [23].

Phylogenetic analysis of ITS and LSU sequence data from *M. scaettae* confirmed its placement within Phaeosphaeriaceae (class Dothideomycetes; order Pleosporales). This is a large and complex family comprising ca. 80 genera and >400 species, including many plant pathogenic species (mainly on monocotyledonous hosts), which has undergone several recent revisions Li et al., 2016; [21], as large-scale DNA barcoding projects have led to revision of many species and the naming of new taxa. *M. scaettae* is, however, unusual in that it readily forms arthroconidia in culture and that no known sexual stage is known [24].

Considering the absence of ITS sequence variation within *M. scaettae* populations, we sought to employ an approach which highlighted chemical and therefore possibility functional differences between the strains. FTIR chemical fingerprinting has been extensively used to identify bacterial species [25] including clinically relevant pathogenic forms [26,27] and also fungi [28–30].

Our FTIR analyses suggest the utility of this approach in fungal classification with discrimination observed amongst strains where metabolite fingerprints appeared to show difference between strains originated from male and female flowers, this could reflect some specialisation required to infect particular types of spathe, and possibly through the production of certain toxins.

How far these reflect genetic differences is unclear but *M. scaettae* does not appear to be particularly subtle flower-infecting pathogen. In the classification of floral pathogens, *M. scaettae* belongs to group 1 being an unspecialized pathogens causing necrotic symptoms and includes such as blossom blights. These fungi typically attack other aboveground plant parts and complete multiple spore cycles during the season. When flowers are infected, necrotic symptoms result and the fungus usually sporulates asexually on affected tissues. Blossom blights caused by *Botrytis* and *Monilinia* species are typical examples [31]. It is possible that the FTIR results represent a metabolic memory of infecting different flower organs. If this were the case, this memory was maintained over successive rounds of culture on PDA, possibly through some epigenetic imprinting.

The absence of any variation in the ITS region based on the sequences from the current study, as well as published sequences from Spain and Iraq, suggests that the sexual stage of *M. scaettae* may be rare or absent, and possibly that the disease is relatively recent in origin. However [32], have recently reported that some simple sequence repeats (SSR; microsatellite) markers, developed for the closely related fungus *Phaeosphaeria nodorum* ('Septoria' blotch of wheat), yield amplification products in *M. scaettae*. Using these SSR markers, they

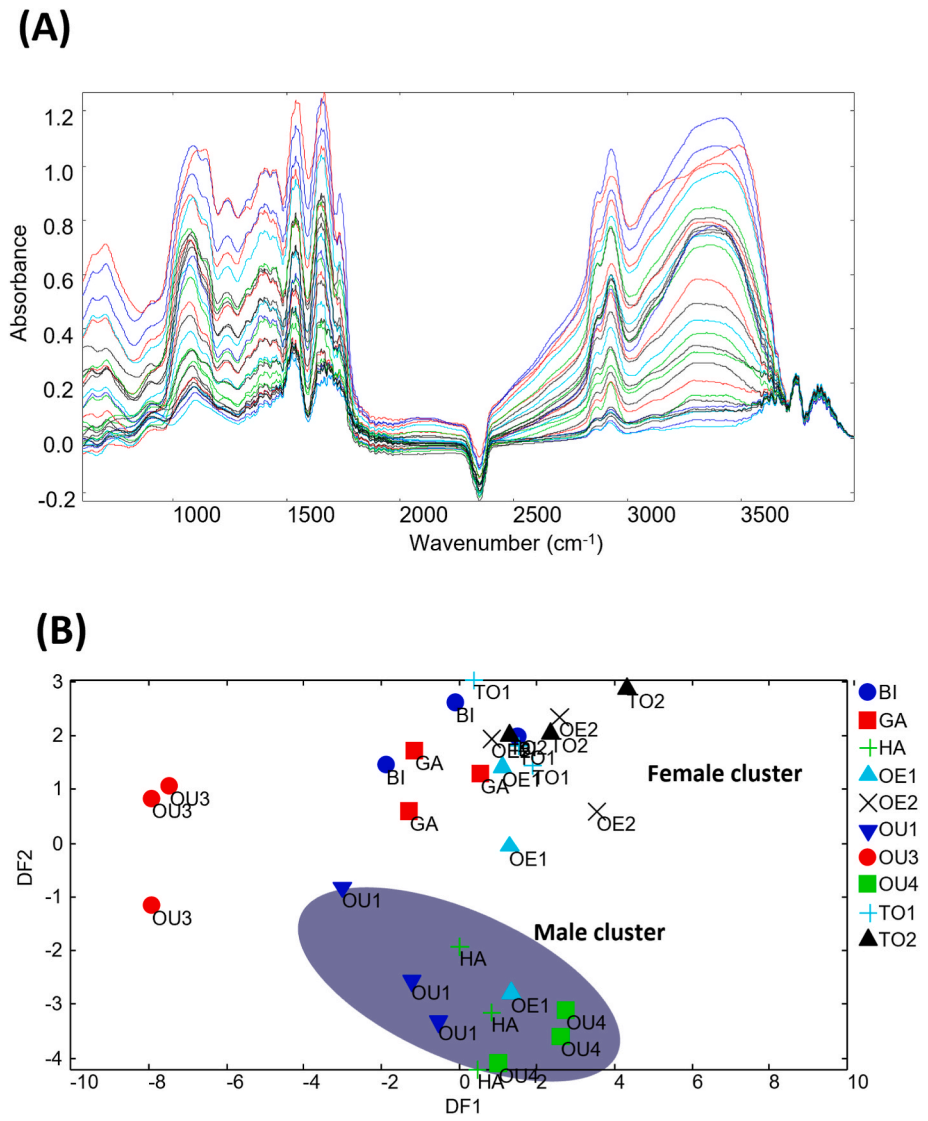

Fig. 5. Metabolite fingerprinting *Mauginiella scaettae* isolates using FTIR spectroscopy. (A) Typical FTIR spectra obtained from mycelia of *M. scaettae* strains (B) Discriminant Function Analysis (DFA) of FTIR spectra based on 4 principal components (PC) explaining 96.5% of the total variation. Two clusters are indicted encompassing fingerprints obtained from either female or male spathe. (filled blue oval added to aid viewing).

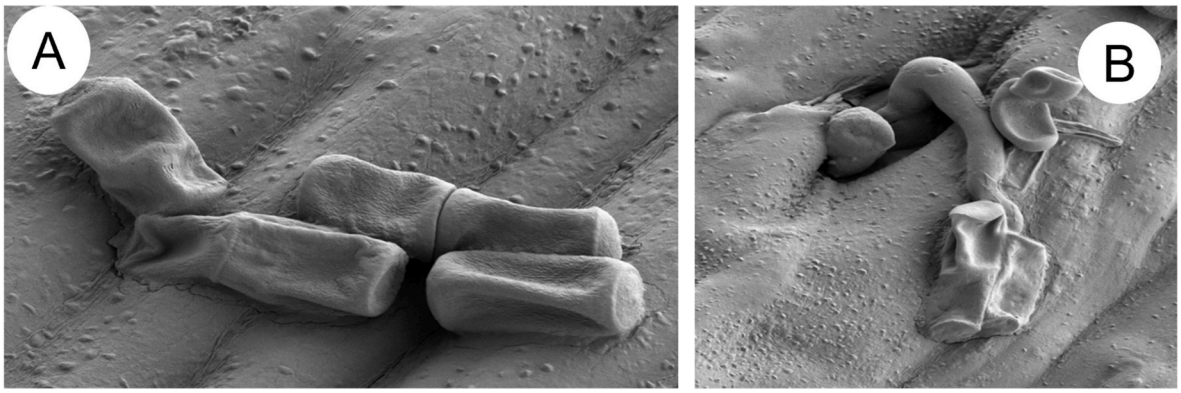

Fig. 6. The infection strategy of *Mauginiella scaettae*. Scanning electron microscopy (SEM) micrograph of the surface of inflorescence rot exhibited date palm showing (A) distinctive arthrocondia and (B) a germinated arthrocondium demonstrating penetration of the host via a stoma. Magnification 500 x .

detected geographical variation within Iranian populations of *M. scaettae*. It would be useful to extend such studies to *M. scaettae* populations in Algeria in order to confirm our phenotypic analyses based on FTIR spectra.

Taking our observations together, *M.scaettae* is confirmed to be a major causal agent in the formation of date inflorescence rot. It is placed

in the family to the Phaeosphaeriaceae which includes many species pathogenic to monocotolydonous hosts. We suggest that *M. scaettae* should be the focus of appropriate monitoring programmes, targeted fungicide use and the long term replacement of date palm stands with resistant germplasm.

Declaration of competing interest

The authors declare that they have no known competing financial interests or personal relationships that could have appeared to influence the work reported in this paper.

Data availability

Data will be made available on request.

Acknowledgements

The authors are grateful for PhD scholarships to MB and BD (Aber-Doc, UK).

Appendix A. Supplementary data

Supplementary data to this article can be found online at https://doi.org/10.1016/j.pmpp.2023.102062.

References

[1] FAOSTAT, Crop Production 2018, Statistics Division, Food and Agriculture Organization of the United Nations, 2020.
[2] M. Djerbi, New records of date palm disease in the United Arab Emirates and Bahrain, Date Palm J. 1 (1982) 307–308.
[3] R.C. Ploetz, D. Ohr Howard, J.B. Carpenter, Y. Pinkas, Disease of date, in: R. C. Ploetz (Ed.), *Diseases Of Tropical Fruits Crops* (Pp235-236), CAB publishing, 2003, https://doi.org/10.1079/97808519939040000.
[4] F. Cavara, Atrofia fiorale in *Phoenix dactylifera* L, di Cirenacia Atti Reale Accademia Nazionale dei Lincei series 6 (1925) 65–67.
[5] F. Cavara, *Mauginiella scaettae* Cav. nuovo ifomicete parassita della palma da datteri in virenacia, Bollettino del Real Orto Botanico di Napoli 8 (1925) 207–211.
[6] R. Maire, R.G. Werner, Fungi maroccani, Mémoires de la Société des Sciences Naturelles du Maroc 45 (1937) 1–147.
[7] P. Munier, L'assaba, Essai Monographique, Saint- Louis, Senegal, Centre ifanmauritanie. Études Mauritaniennes, 1952, p. 72, 3.
[8] P. Munier, Le palmier dattier en Mauritanie, Annales de l'Institut des Fruits et Agrumes (IFAC) 12 (1955) 66p.
[9] S.S. Rattan, A.H.A. AL-Dboon, Notes on fungi associated with date palm I, Sydowia 32 (1980) 246–273.
[10] I.F. Michael, K.A. Sabet, Biology and control of *Mauginiella scaettae* Cav, the pathogen of Khamedj disease in the united Arab Republic, Annual Date Grower's Institue 47 (1970) 5–8.
[11] F. Hussain, Occurrence of date palm inflorescence rot in Iraq, Plant Dis. Rep. 42 (1958) 555.
[12] T.J. White, T. Bruns, S. Lee, J. Taylor, Amplification and direct sequencing of fungal ribosomal RNA genes for phylogenetics, in: M.A. Innis, H. Gelfand, J. S. Sninsky, T.J. White (Eds.), PCR Protocols. Guide to Methods and Applications, Academic Press, 1990, pp. 315–322.
[13] A.J. Drummond, B. Ashton, S. Buxton, M. Cheung, A. Cooper, C. Duran, M. Field, J. Heled, M. Kearse, S. Markowitz, R. Moir, S. Stones-Havas, S. Sturrock, T. Thierer, Wilson, Geneious V556, 2012. http://www.geneious.com/.
[14] K. Katoh, K. Misawa, K. Kuma, T. Miyata, MAFFT: a novel method for rapid multiple sequence alignment based on fast Fourier transform, Nucleic Acids Res. 30 (14) (2002) 3059.
[15] S. Guindon, J.F. Dufayard, V. Lefort, M. Anisimova, W. Hordijk, O. Gascuel, New algorithms and methods to estimate maximum-likelihood phylogenies: assessing the performance of PhyML30, Syst. Biol. 59 (3) (2010) 307–321. https://doiorg/101093/sysbio/syq010.
[16] E. Gidman, R. Goodacre, B. Emmett, A.R. Smith, D. Gwynn-Jones, Investigating plant-plant interference by metabolic fingerprinting, Photochemistry 63 (2003) 705–710, https://doi.org/10.1016/S0031-9422(03)00288.
[17] E.M. Timmins, S.A. Howell, B.K. Alsberg, W.C. Noble, R. Goodacre, Rapid differentiation of closely related *Candida* species and strains by pyrolysis-mass spectrometry and Fourier transform-infrared spectroscopy, J. Clin. Microbiol. 36 (1998) 367–374, https://doi.org/10.1128/JCM362367-3741998.
[18] R. Goodacre, D. Broadhurst, A.K. Smilde, S. Bruce, B.S. Kristal, J.D. Baker, R. Beger, C. Bessant, S. Connor, G. Capuani, A. Craig, T. Ebbels, D.B. Kell, C. Manetti, J. Newton, G. Paternostro, R. Somorjai, M. Sjöström, J. Trygg, F. Wulfert, Proposed minimum reporting standards for data analysis in metabolomics, Metabolomics 3 (2007) 231–241, https://doi.org/10.1007/s11306-007-0081-3.
[19] H.J.H. MacFie, C.S. Gutteridge, J.R. Norris, Use of canonical variates in differentiation of bacteria by pyrolysis gas-liquid chromatography, J. Gen. Microbiol. 104 (1978) 67–74, https://doi.org/10.1099/00221287.
[20] W. Windig, J. Haverkamp, P.G. Kistemaker, Interpretation of sets of pyrolysis mass spectra by discriminant analysis and graphical rotation, Anal. Chem. 55 (1) (1983) 81–88, https://doi.org/10.1021/ac00252a023.
[21] D.S. Tennakoon, K.M. Thambugala, D.N. Wanasinghe, E. Gentekaki, I. Promputtha, C.H. Kuo, K.D. Hyde, Additions to Phaeosphaeriaceae (Pleosporales): Elongaticollum gen. nov., *Ophiosphaerella taiwanensis* sp. nov., *Phaeosphaeriopsis beaucarneae* sp. nov. and a new host record of *Neosetophoma poaceicola* from Musaceae, MycoKeys 70 (2020) 59.
[22] M.A. Hameed, Inflorescence rot disease of date palm caused by *Fusarium proliferatum* in Southern Iraq, Afr. J. Biotechnol. 11 (35) (2012) 8616–8621, https://doi.org/10.5897/AJB12471.
[23] J. Chong, D.E. Harder, R. Rohringer, Cytochemical studies on *Puccinia graminis* f. sp. *tritici* in a compatible wheat host II Haustorium mother cell walls at the host cell penetration site, haustorial walls, and the extrahaustorial matrix, Can. J. Bot. 64 (11) (1986) 2561–2575, https://doi.org/10.1139/b86-339.
[24] Ariyawansa, et al., Fungal diversity notes 111–252—taxonomic and phylogenetic contributions to fungal taxa, Fungal Divers. 75 (2015) 27–274.
[25] J.J. Ojeda, M. Dittrich, Fourier transform infrared spectroscopy for molecular analysis of microbial cells, Methods Mol. Biol. 881 (2012) 187–211, https://doi.org/10.1007/978-1-61779-827-6_8.
[26] B. Dziuba, A. Babuchowski, D. Nalecz, M. Niklewiczb, Identification of lactic acid bacteria using FTIR spectroscopy and cluster analysis, Int. Dairy J. 17 (2007) 183–189, https://doi.org/10.1016/jidairyj200602013.
[27] P. Zarnowiec, L. Lechowicz, G. Czerwonka, W. Kaca, Fourier transform infrared spectroscopy (FTIR) as a tool for the identification and differentiation of pathogenic bacteria, Curr. Med. Chem. 22 (14) (2015) 1710–1718. https://doiorg/102174/092986732266615031115280O.
[28] C. Santos, M.E. Fraga, Z. Kozakiewicz, N. Lima, Fourier transform infrared as a powerful technique for the identification and characterization of filamentous fungi and yeasts, Research inMicrobiology 161 (2) (2010) 168–175, https://doi.org/10.1016/j.resmic.2009.12.007.
[29] A. Lecellier, J. Mounier, V. Gaydou, L. Castrec, G. Barbier, W. Ablain, M. Manfait, D. Toubas, G.D. Sockalingum, Differentiation and identification of filamentous fungi by high- throughput FTIR spectroscopic analysis of mycelia, Int. J. Food Microbiol. (2014) 32–41, https://doi.org/10.1016/jijfoodmicro201310011, 168-169.
[30] A. Lecellier, V. Gaydou, J. Mounier, A. Hermet, L. Castrec, G. Barbier, W. Ablain, M. Manfait, D. Toubas, G.D. Sockalingum, Implementation of an FTIR spectral library of 486 filamentous fungi strains for rapid identification of molds, Food Microbiol. 45 (2015) 126–134, https://doi.org/10.1016/jfm201401002. Part A.
[31] H.K. Ngugi, H. Scherm, Biology of flower-infecting fungi, Annu. Rev. Phytopathol. 44 (2006) 261–282, https://doi.org/10.1146/annurev.phyto.44.070505.143405.
[32] H. Alvanipour, H. Aminian, K. Alami-Saeid, K. Sorkheh, R. Farrokhinejad, A. Nejati, M. Javan- Nikkhah, Cross-transferability of SSR loci of *Phaeosphaeria nodorum* to *Mauginiella scaettae*, Mycologia Iranica 7 (1) (2020) 135–142.